Adsorption (2024) 30:1239–1249
https://doi.org/10.1007/s10450-024-00505-3

RESEARCH ARTICLE

Selective adsorption of ethane and methane on zeolite-like imidazolate frameworks ZIF-8 and ZIF-67: effect of lattice coordination centers

G. S. Deyko[1] · V. I. Isaeva[1] · L. M. Glukhov[1] · V. V. Chernyshev[2,3] · D. A. Arkhipov[1] · G. I. Kapustin[1] · L. A. Kravtsov[1,2] · L. M. Kustov[1,2]

Received: 21 March 2024 / Revised: 28 May 2024 / Accepted: 1 June 2024 / Published online: 9 June 2024

Abstract

Zeolitic imidazolate frameworks based on 2-methylimidazolate linkers with different particle size (200–1000 nm) and controlled content of Zn^{2+} and Co^{2+} ions have been synthesized by microwave (MW) assisted technique according to original procedures and room-temperature method. The produced materials including monometallic ZIF-8 and ZIF-67 samples, bimetallic ZIF-Zn/Co (or ZIF-8/ZIF-67) system, and "core-shell" ZIF-8@ZIF-67 and ZIF-67@ZIF-8 composites have been studied in the practically relevant process of selective adsorption of ethane and methane (25 °C). The adsorption isotherms for both gases on the obtained ZIF materials were measured in a wide pressure range (1–20 atm) for the first time. For ZIF-67, the isosteric heats of adsorption for both gases were obtained also for the first time. It was found that the nature of the coordination centers in the ZIF frameworks influences their adsorption characteristics. Thus, the obtained materials with Co^{2+} ions show an increased adsorption capacity towards ethane, which exceEDX the capacity measured for the Zn^{2+}-based samples, while the highest methane adsorption value is achieved on a "core-shell" ZIF-67@ZIF-8 composite.

Keywords Metal-organic frameworks · Zeolite-like imidazolate frameworks · Selective adsorption · Ethane · Methane

The development of advanced methods of ethane separation from natural gas is an extremely important task. Among them, the adsorption on porous solids presents an energy-saving and highly efficient technique. A new type of hybrid nanoporous materials - metal-organic frameworks (MOFs) - shows a special potential as efficient ethane adsorbents. They are crystalline porous coordination polymers composed of metal ions or small clusters connected by polydentate organic molecules (linkers). MOFs are characterized by high specific surface area and porosity, as well as a fully open pore system. Their important feature is a possibility of fine tuning of the framework structure, pore geometry and functionality by rational selection of metal ions and organic linkers for the specific process, particularly gas adsorption.

It is known that metal ions (coordination centers) in MOF matrices can serve as adsorption sites for "guest" molecules [1]. To study in details an impact of the coordination center (metal ions) in the framework on its adsorption performance, the zeolitic imidazolate framework ZIF-8 ($Zn(MIM)_2$, MIM = 2-methylimidazolate) and its isostructural analog ZIF-67 ($Co(MIM)_2$) are valuable model systems. Both materials belong to the particular ZIF family (a subclass of a large MOF class). Their frameworks with a sodalite-like topology contain cavities with a diameter of 11.6 Å, accessible through "windows" with diameters of 3.4 Å (ZIF-8) and 3.3 Å (ZIF-67) [2]. The difference in the window sizes is due to the fact that the Co-N bond in the ZIF-67 matrix is shorter than the Zn-N bond in the ZIF-8 matrix) [3]. ZIF-8 and ZIF-67 matrices exhibit framework mobility

✉ G. S. Deyko
gdeyko@gmail.com

[1] Zelinsky Institute of Organic Chemistry, Russian Academy of Sciences, Leninsky Prospekt 47, Moscow 119991, Russia

[2] Department of Chemistry, Lomonosov Moscow State University, Leninskie Gory 1-3, Moscow 119991, Russia

[3] A.N. Frumkin Institute of Physical Chemistry and Electrochemistry, Russian Academy of Sciences, Leninsky Prospekt 31, p. 4, Moscow 119071, Russia

or flexibility, which allows "guest" adsorbate molecules to diffuse into their intracrystalline space [4], with faster diffusion being observed for small gas molecules [2]. However, the ZIF-67 framework is more rigid than ZIF-8 one.

The cavities in the ZIF-8 structure can accommodate relatively large molecules, such as benzene [5]. This effect is related to the ability of the framework to stretch or open "windows" due to the mobility (ability to rotate) of 2-MIM linkers forming the framework, which was shown by ^{2}H NMR method [5].

Obviously, the differences in the flexibility of ZIF-8 and ZIF-67 frameworks and the diameter of "windows" affect the adsorption behavior of these materials. In particular, it was demonstrated by computational methods that ZIF-67 has improved separation efficiency towards ethane in ethylene/ethane mixture compared to ZIF-8 [4]. The reason is the more rigid framework and smaller pore diameter of ZIF-67 compared to ZIF-8. The increased rigidity of the ZIF-67 framework is indicated by the fact that nitrogen adsorption at 77 K (based on the "window opening" effect caused by the rotation of the MIM linker) begins for ZIF-67 at a slightly higher pressure (1.0×10^{-2} Pa) than for its analog ZIF-8 (0.6×10^{-2} Pa) [3].

It is known that there are a number of isostructural compounds $[Zn_xCo_{1-x}(MIM)_2]$ with ZIF-8 structure, which include both Zn^{2+} and Co^{2+} ions in the frameworks [6]. This fact allows us to compare the adsorption properties of such materials differing in the composition of their inorganic block (Co^{2+} ion content), since they have similar textural properties. In the same work, the adsorption of CO_2, N_2, and CH_4 was studied on a series of $[Zn_xCo_{1-x}(MIM)_2]$ samples, and it was shown that introducing Co^{2+} ions into the ZIF-8 structure significantly impacts the equilibrium adsorption values for these gases [6]. In Ref [7]. , bimetallic nanoparticles $[Zn_{0.5}Co_{0.5}(MIM)_2]$ were deposited on porous aluminum oxide under microwave activation. The prepared composite membrane showed a remarkably higher separation factor for propylene/propane gas mixture (120) than its ZIF-8 counterpart. The authors also attributed the improved separation properties of the bimetallic sample to the smaller pore diameter and increased rigidity of the adsorbent framework compared to the monometallic carrier [7].

Zn/Co-ZIF bimetallic nanoparticles (ZIF-8/ZIF-67) used as a nanofiller for the cross-linked poly(ethylene oxide)-based mixed matrix membranes (MMMs) improve the separation of CO_2/N_2 and CO_2/H_2 gas mixtures. In particular, these MMMs show higher CO_2 diffusion coefficient and solubility, and increased Robeson upper bound (2008) due to π-complexation between Zn^{2+}, Co^{2+} ions and CO_2 molecules. The transport of gas molecules inside the ZIF-8/ZIF-67 bimetallic matrix is facilitated by the low diffusion resistance of the framework channels [3].

Other type of bimetallic adsorbents in form of the core-shell MOF@MOF composites based on ZIF-8 and ZIF-67 materials are well described in the literature [8, 9]. These nanostructures are formed by creating a "shell" over previously synthesized particles ("core"). The peculiarities of their nitrogen adsorption behavior at 77 K were studied [3]. It was found that the pressure at which the adsorption starts differs from the values for the individual ZIF-8 and ZIF-67 components, as well as for their mechanical mixture due to the opening of "windows" for the ZIF-8@ZIF-67 composite (ZIF-8 "core", ZIF-67 "shell"). According to the authors, this phenomenon is due to the cooperative effect of MIM linker rotation. On the contrary, the adsorption behavior of the ZIF-67@ZIF-8 carrier (ZIF-67 "core", ZIF-8 "shell") corresponds to the behavior of the mechanical mixture of both components. In the case of ZIF-67@ZIF-8 composite, the cooperative effect of simultaneous rotation of "core" and "shell" linkers is not realized due to the weak contact between ZIF-67 and ZIF-8 domains in this nanostructure.

The composite materials ZIF-8@ZIF-67 and ZIF-67@ZIF-8 show enhanced adsorption capacity towards carbon dioxide and hydrogen compared to their individual components ZIF-8 and ZIF-67 [10]. Similar composites in the form of nanoparticles have also been used as a filler for the fabrication of MMMs, which exhibit improved selectivity for hydrogen in the separation of H_2/CH_4 and H_2/N_2 gas mixtures [2]. However, there is no information in the literature on the adsorption of methane and ethane on ZIF-8@ZIF-67 and ZIF-67@ZIF-8 materials.

Taking into account the literature data, this study is aimed at an elucidation of the role of coordination centers - metal ions (Zn^{2+} and Co^{2+}) - in ZIF matrices on their capacity and selectivity in the adsorption of the main components of natural gas - methane and ethane. For this, a series of the sodalite-like ZIF materials, i.e., ZIF-8, ZIF-67, bimetallic ZIF-Zn/Co systems containing Zn^{2+} and Co^{2+} ions at molar ratios of 1 : 2, 1 : 1, 2 : 1, as well as "core-shell" ZIF-8@ZIF-67 and ZIF-67@ZIF-8 composites were synthesized and characterized in detail by physicochemical methods, i.e., pXRD analysis, DRIFTS, SEM, EDX-SEM, low temperature N_2 adsorption, and elemental analysis (ICP-MS).

1 Experimental

All solvents and reagents used were purified prior to use by standard techniques.

Zn and Co content in the obtained materials was determined by inductively coupled plasma-mass spectrometry (ICP-MS) in the microanalysis laboratory of NUST "MISiS".

Optimization of analytical SEM measurements was carried out within the framework of the approach described earlier [11]. Prior to imaging, samples were placed on the surface of a 25 mm diameter aluminum stage, fixed with conductive tape and sputtered with a 10 nm thick conductive metal layer (Au/Pd, 60/40) by magnetron sputtering method [12]. The microstructure of the samples was studied by field emission scanning electron microscopy (FE-SEM) on a Hitachi SU8000 electron microscope. Image acquisition was carried out in the mode of secondary electron registration at an accelerating voltage of 10 kV. The morphology of the samples was studied taking into account the correction for the surface effects of sputtering the conductive layer [12]. To study the samples by X-ray microanalysis (EDX-SEM), they were placed on the surface of an aluminum table with a diameter of 25 mm, fixed with conductive plasticine and sputtered with a conductive carbon layer with a thickness of 10 nm. The study was performed using an Oxford Instruments X-max 80 energy dispersive X-ray spectrometer at an accelerating voltage of 20 kV.

The powder diffraction patterns were measured in the 5–40° 2θ range at room temperature on the EMPYREAN laboratory diffractometer (PANalytical, Malvern, UK) (Ni-filtered Cu*Kα* radiation) equipped with X'celerator linear detector. Instrument parameters are: X-ray tube voltage/current 40 kV/35 mA, divergence slits 1/4 and 1/2°, scan rate 0.2° min^{-1}.

The characteristics of the porous structure of the synthesized materials were determined using the standard adsorption isotherm of N_2 vapor at 77 K measured on an ASAP 2020 Plus instrument (Micromeritics). The specific surface area (A_{BET}) of the samples was calculated in accordance with ISO 9277 standard (relative pressure range 0.003–0.03). The total pore volume (V_{tot}.) was estimated at $p/p^o = 0.99$. The micropore volume(V_μ) was estimated using the "*t-plot* method". The mesopore volume was calculated as the difference between V_{tot} and V_μ.

ZIF-67, ZIF-8 and bimetallic ZIF-Zn/Co samples were synthesized according to the original procedures using a MW-activation of the reaction mass at atmospheric pressure.

1.1 ZIF-67

A solution of $Co(CH_3COO)_2 \cdot 4H_2O$ (0.75 g, 3.0 mmol) was added to a solution of 2-methylimidazole (8.2 g, 100 mmol) in water (90 mL). The combined solution was placed in a reactor for MW-synthesis (30 min, 200 W). The reaction product was separated by centrifugation, washed with distilled water (3 × 15 mL) and methanol (3 × 15 mL). The obtained purple crystals were dried in air (2 h, 60 °C) and then activated in *vacuo* (8 h, 150 °C). The yield of the product was 0.40 g (~60%).

1.2 ZIF-8

A solution of $Zn(CH_3COO)_2 \cdot 2H_2O$ (0.66 g, 3.0 mmol) was added to a solution of 2-methylimidazole (8.2 g, 100 mmol) in water (90 mL). The combined solution was placed in a reactor for microwave synthesis (30 min, 200 W). The reaction product was separated by centrifugation, washed with distilled water (3 × 15 mL) and methanol (3 × 15 mL). The obtained purple crystals were dried in air (2 h, 60 °C) and then activated in *vacuo* (8 h, 150 °C). The yield of the product was 0.45 g (~66%).

1.3 ZIF-Zn/Co (1 : 1)

A solution of $Co(CH_3COO)_2 \cdot 4H_2O$ (0.87 g, 3.0 mmol) and $Zn(CH_3COO)_2 \cdot 4H_2O$ (0.26 g, 1 mmol) in water (180 mL) was added to a solution of 2-methylimidazole (1.968 g, 24 mmol) in water (90 mL). The combined solution was placed in a reactor for microwave synthesis (30 min, 200 W). The reaction product was separated by centrifugation, washed with distilled water (3 × 15 mL) and methanol (3 × 15 mL). The obtained purple crystals were dried in air (2 h, 60 °C) and then activated in *vacuo* (6 h, 140 °C). The yield of the product was 0.85 g (~94%).

1.4 ZIF-Zn/Co (1 : 2)

A solution of $Co(CH_3COO)_2 \cdot 4H_2O$ (0.988 g, 4.0 mmol) and $Zn(CH_3COO)_2 \cdot 2H_2O$ (0.44 g, 2 mmol) in water (60 mL) was added to a solution of 2-methylimidazole (8.2 g, 100 mmol) in water (90 mL). The combined solution was placed in a reactor for microwave synthesis (30 min, 200 W). The reaction product was separated by centrifugation, washed with distilled water (3 × 15 mL) and methanol (3 × 15 mL). The obtained purple crystals were dried in air (2 h, 60 °C) and then activated in *vacuo* (6 h, 140 °C). The yield of the product was 0.80 g (~60%).

1.5 ZIF-Zn/Co (2 : 1)

A solution of $Co(CH_3COO)_2 \cdot 4H_2O$ (0.494 g, 2.0 mmol) and $Zn(CH_3COO)_2 \cdot 2H_2O$ (0.88 g, 4 mmol) in water (60 mL) was added to a solution of 2-methylimidazole (8.2 g, 100 mmol) in water (90 mL). The combined solution was placed in a reactor for microwave synthesis (30 min, 200 W). The reaction product was separated by centrifugation, washed with distilled water (3 × 15 mL) and methanol (3 × 15 mL). The obtained purple crystals were dried in air (2 h, 60 °C) and then activated in *vacuo* (6 h, 140 °C). The yield of the product was 0.79 g (~59%).

"Core-shell" samples were synthesized using modified method described in Ref [8].

1.6 ZIF-67@ZIF-8 (Co : Zn = 1 : 1)

The preliminary synthesized ZIF-67 sample (0.5 g) was suspended in methanol (33 mL). Then, $Zn(CH_3COO)_2 \cdot 2H_2O$ (4.39 g, 20 mmol) was dissolved in methanol (33 mL) and the resulting solution was added under stirring to the ZIF-67 suspension, followed by the solution of 2-methylimidazole (6.15 g, 75 mmol) in methanol (33 mL). The resulting mixture was stirred for 24 h at 22 °C. The reaction product was isolated *via* centrifugation, washed with distilled water (3 × 15 mL) and methanol (3 × 15 mL). The resulting powder was dried in air (2 h, 60 °C), and then in *vacuo* (6 h, 140 °C). The yield of the product was 1.00 g (~93%).

1.7 ZIF-8@ZIF-67 (Zn : Co = 1 : 1)

This sample was synthesized similarly to the above procedure using ZIF-8 as a "core". $Co(CH_3COO)_2 \cdot 4H_2O$ was used as a source of Co^{2+} ions for "shell" taken in the amounts necessary to provide the same metal ion : MIM molar ratio. The yield of the product was 1.00 g (~91%).

The adsorption of methane and ethane was measured using a volumetric adsorption apparatus (Sieverts method). The setup and the measurement methodology are described in detail in Ref [13].

The isosteric heat of adsorption of the investigated gases was determined in the temperature range 0–75 °C from the adsorption isotherms for methane and ethane obtained at temperatures 0, 25, 50 and 75 °C, by the following formula (1) [14]:

$$q_{st.} = -RZ\left(\frac{\partial\,(ln\ p)}{\partial\left(\frac{1}{T}\right)}\right)_a \tag{1}$$

where a is the adsorption value, p is the equilibrium pressure, Z is the compressibility coefficient at a given temperature and pressure, and R is the universal gas constant.

IAST selectivity values for ethane/methane pair were calculated using the Ideal Adsorbed Solution Theory (IAST) according to [15] and [16]. The calculations were performed for a mixture of methane with 10 mol% ethane, as the closest in composition to natural gas ($y_{C_2H_6}$= 0.1 и $y_{?H_4}$= 0.9).

The ideal selectivity for the C_2H_6/CH_4 pair was determined using formula (2):

$$S_{ideal}\,(P,T) = \frac{a_{C_2H_6}\,(P,T)}{a_{CH_4}\,(P,T)} \tag{2}$$

where $a_{C_2H_6}(P,T)$ и $a_{CH_4}(P,T)$ are adsorption values calculated from experimental isotherms by B-spline interpolation.

Table 1 Elemental analysis data for the ZIF-based materials

Material	w(Co), %	w(Zn), %	w(Co), mol%
ZIF-Zn/Co (Zn : Co = 2 : 1)	8.7*	17.1*	36.0*
ZIF-Zn/Co (Zn : Co = 1 : 2)	16.5*	9.7*	65.3*
ZIF-Zn/Co (Zn : Co = 1 : 1)	12.5	13.6	50.5
ZIF-67@ZIF-8	13.7	12.9	54.1
ZIF-8@ZIF-67	12.2	14.8	47.7

*The values were obtained from SEM-EDX data

2 Results and discussion

To study an effect of the coordination center in the adsorbent framework on the adsorption of methane and ethane, ZIF-8, ZIF-67, bimetallic ZIF-Zn/Co (Zn : Co = 1 : 2, 1 : 1, and 2 : 1) samples were obtained by an original MW-assisted procedure at atmospheric pressure. The "core-shell" ZIF-8@ZIF-67 (Zn : Co = 1 : 1) and ZIF-67@ZIF-8 (Co : Zn = 1 : 1) composites were synthesized by RT procedure. In this case, the pre-synthesized ZIF-8 or ZIF-67 samples were used as "cores" for the room-temperature synthesis of ZIF-8 or ZIF-67 "shells", respectively.

The data on the zinc and cobalt contents in the bimetallic and "core-shell" samples (determined by ICP-MS) are summarized in Table 1.

According to the elemental analysis (EA) data (Table 1), the zinc and cobalt contents in ZIF-Zn/Co sample (atom ratio Zn : Co = 1 : 1) are approximately the same. However, for the "core-shell" ZIF-8@ZIF-67 and ZIF-67@ZIF-8 composites, the ratio of Zn^{2+} and Co^{2+} ions is determined by the type of the "core". So, the "core-shell" ZIF-67@ZIF-8 material contains 8% more Co^{2+} ions, and ZIF-8@ZIF-67 has 5% more Zn^{2+} ions. Apparently, the reaction yield decreases when the corresponding "shell" is formed, due to the presence of the pre-synthesized composite "core" in the reaction mixture. A similar phenomenon has been reported in the literature [9].

EDX-SEM results (Figs. S1-S5) for bimetallic ZIF-Zn/Co and "core-shell" ZIF-8@ZIF-67 and ZIF-67@ZIF-8 samples are in a good accordance with EA data. They show also a homogeneous Zn and Co distribution on the surface of bimetallic materials.

2.1 Structural examinations of the synthesized ZIF adsorbents

The experimental powder diffraction patterns for all samples are shown in Fig. 1. All diffraction peaks on each pattern correspond to a standard cubic crystal structure specific

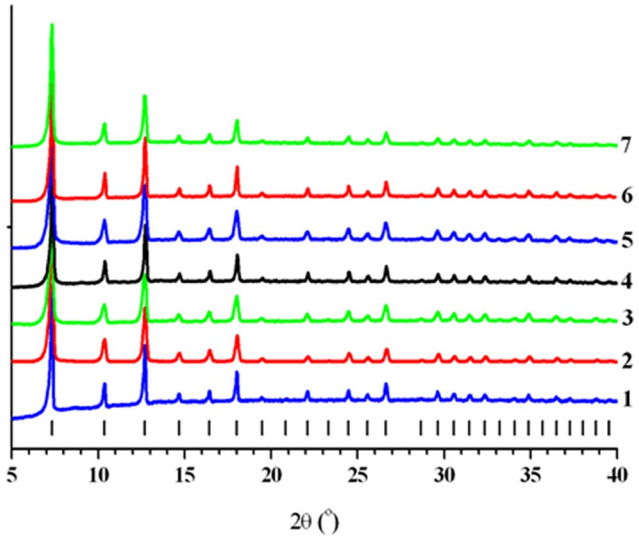

Fig. 1 X-ray powder diffraction patterns of the samples ZIF-67 (**1**), ZIF-8 (**2**), ZIF-Zn/Co (Zn : Co = 2 : 1) (**3**), ZIF-Zn/Co (Zn : Co = 1 : 2) (**4**), ZIF-Zn/Co (Zn : Co = 1 : 1) (**5**), "core-shell" ZIF-67@ZIF-8 (**6**) and "core-shell" ZIF-8@ZIF-67 (**7**). The vertical black bars correspond to the calculated positions of the Bragg peaks for the cubic unit cell ($a = 17.04$ Å) and space group *I-43m*

to ZIF-8 and ZIF-67 frameworks. As an illustrative example, the Pawley [17] fitting performed using the MRIA program [18] for the ZIF-Zn/Co (Zn : Co = 1 : 2) sample led to $\chi^2 = 1.08$ (see Fig. S4) for the space group *I-43 m* and cubic unit cell parameter $a = 17.052(2)$ Å. The values of parameter a for all samples obtained in the similar fittings have no significant differences and are lying in the range 17.012(2) – 17.052(2) Å (see also Table S1). At the same time, there are visible differences in the width of the peaks for the samples with opposite ratio of Zn and Co atoms. Comparing the powder patterns of the ZIF-8 (Zn only) and ZIF-67 samples (Co only) one can see that the width of the peaks of the ZIF-8 materials is greater than that of ZIF-67 sample (Fig. S7), which means that the ZIF-67 crystallites are significantly larger than the crystallites ZIF-8. The same conclusion follows from the comparison of XRD patterns of samples ZIF-Zn/Co (Zn : Co = 2 : 1) and ZIF-Zn/Co (Zn : Co = 1 : 2) (Fig. S8), and "core-shell" ZIF-8@ZIF-67 and ZIF-67@ZIF-8 (Fig. S9), where the Zn : Co ratio is > 1 in the former sample and < 1 in the latter sample, respectively. This observation is in a good accordance with SEM results, i.e., the crystallites of the Co-containing samples are larger than that of the Zn-containing ones.

2.2 Morphology of the ZIF adsorbents

The synthesized ZIF materials crystallize in the form of submicron-sized particles (Fig. 2). Monometallic samples consist of regular octahedron shaped crystals (Fig. 2a, b) with the size of 0.8-1.0 µm (ZIF-67) and 190–260 nm (ZIF-8). The bimetallic ZIF-Zn/Co (Zn : Co = 1 : 1) material has

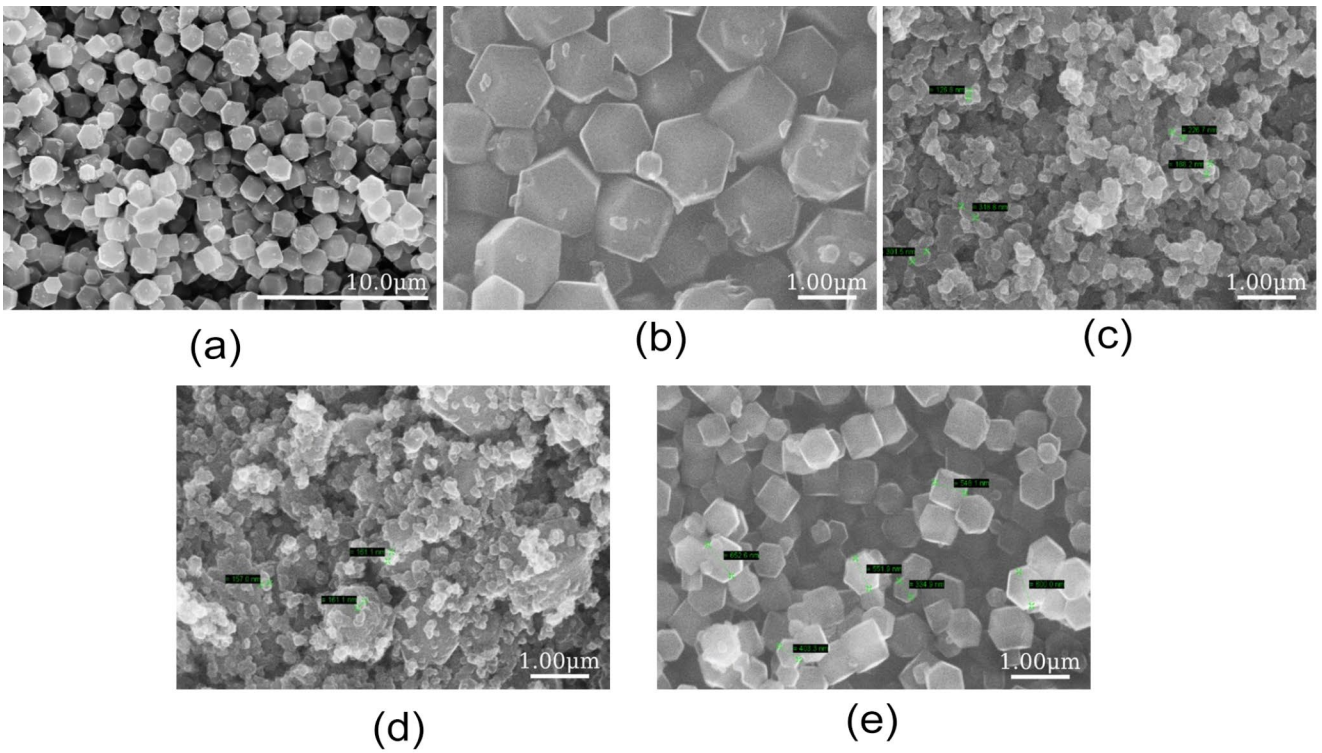

Fig. 2 SEM micrographs of ZIF-8 (**a**), ZIF-67 (**b**), "core-shell" ZIF-8@ZIF-67 (**c**), "core-shell" ZIF-67@ZIF-8 (**d**) and ZIF-Zn/Co (Zn : Co = 1 : 1) (**e**) samples

Table 2 Textural characteristics and particle size of the studied materials

Sample	A_{BET}, m^2/g	$V_{tot.}$, cm^3/g	V_{micro}, cm^3/g	V_{meso}, cm^3/g	Pore diameter, nm	Particle size, nm
ZIF-8	1900	0.733	0.643	0.090	0.7–1.7	~190–260
ZIF-67	1844	0.685	0.623	0.062	0.7–1.7	~800–1000
ZIF-Zn/Co (Zn : Co = 1 : 1)	1995	0.746	0.663	0.073	0.7–1.7	~600
ZIF-8@ZIF-67	1986	0.720	0.678	0.042	0.7–1.7	~160
ZIF-67@ZIF-8	1893	0.692	0.658	0.034	0.7–1.7	~230

Table 3 Methane and ethane capacities of the obtained adsorbents (25 °C)

Sample	a(C_2H_6, 1 atm), mmol/g	a(CH_4, 1 atm), mmol/g	a(C_2H_6, 5 atm), mmol/g	a(CH_4, 5 atm), mmol/g	a(C_2H_6, 20 atm), mmol/g	a(CH_4, 20 atm), mmol/g
ZIF-8	2.03	0.30	4.32	1.29	5.54	3.46
ZIF-67	2.29	0.31	5.20	1.43	6.72	4.15
ZIF-Zn/Co (Zn : Co = 1 : 1)	2.23	0.29	4.95	1.32	6.07	3.83
ZIF-67@ZIF-8	2.17	0.73	4.80	2.36	6.09	4.81
ZIF-8@ZIF-67	1.93	0.27	4.29	1.20	5.36	3.35

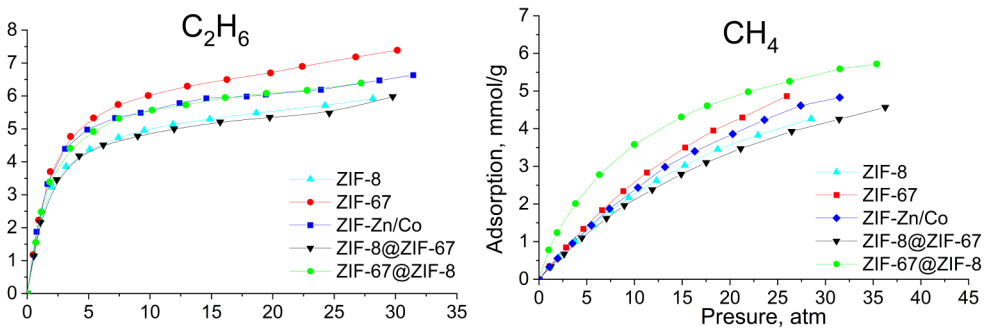

Fig. 3 Methane and ethane adsorption isotherms for the obtained ZIF-based materials (25 °C)

octahedral and cubic shaped particles with intermediate size (~650 nm). The particle size of the "core-shell" ZIF-67@ZIF-8 (Fig. 2, c) and ZIF-67@ZIF-8 (Fig. 2, d) composites is insignificantly reduced in comparison with crystallites forming monometallic and bimetallic materials (Table 2). Thus, the ZIF-8@ZIF-67 system (Fig. 2c) has the smallest crystal size (~160 nm), while the regular octahedral shape of the corresponding "nuclei" (pre-synthesized particles) changes. Apparently, the growth of crystals of the corresponding "shell" framework is simultaneously accompanied by partial degradation of the used "core", which leads to a change both in the average size of the crystallites and their shape.

2.3 Textural characteristics of ZIF materials

The textural characteristics of the studied isostructural ZIF-8, ZIF-67 and ZIF-Zn/Co materials are rather similar (Table 2, Figs. S10-S12). For the monometallic ZIF-8 and ZIF-67 adsorbents, the values of specific surface area are in a good accordance with the literature data ([19, 20]). The bimetallic ZIF-Zn/Co (Zn : Co = 1 : 1) and "core-shell" ZIF-8@ZIF-67 samples show almost identical specific surface areas, which are highest as compared to other materials. However, the textural characteristics of both "core-shell" samples differ very slightly. These differences do not exceed the experimental error of the adsorption method.

2.4 Adsorption properties of the synthesized ZIF materials on methane and ethane

It was found that ZIF-67 sample has a ~20% higher adsorption capacity for methane and ethane (Table 3; Fig. 3) than its isostructural analog ZIF-8 with a bit lower specific surface area and total pore volume (Table 2). The bimetallic ZIF-Zn/Co (Zn : Co = 1:1) material exhibits an ethane adsorption value that is closer to the adsorption value obtained for the ZIF-67 material (Table 3). With respect to methane, these samples show approximately the same adsorption capacity (Fig. 3).

The ethane capacities of the cobalt-containing ZIF-8@ZIF-67, ZIF-67 and ZIF-Zn/Co samples are quite close at a pressure of 1 atm and slightly exceed the capacity of the ZIF-8 material with Zn^{2+} ions (Table 3; Fig. 3). The highest

adsorption value is demonstrated by the ZIF-67 material comprising exclusively Co^{2+} ions as the coordination centers. In the ethane pressure range of 5–20 atm, this trend is more pronounced. An increase in the ethane adsorption capacity for materials containing Co^{2+} ions could be explained by a higher rigidity of the ZIF-67 framework, as well as by the shorter Co-N bond in it as compared to the Zn-N bond in the ZIF-8 framework. These characteristics of cobalt-containing adsorbents provides closer contact of ethane molecule (critical diameter 4 Å) with the pore surface and realization of so-called "commensurate" adsorption. Noteworthy, the same trend of the influence of Co^{2+} ions on the ethane capacity was found out for bimetallic samples ZIF-Zn/Co (1 : 2 and 2 :1 molar rations of metals). So, the ZIF-Zn/Co (1 : 2) sample exhibited higher ethane adsorption value at higher pressure range (> 15 atm) then the ZIF-Zn/Co (2 : 1) one (see Fig. S20).

Extremely close values of methane adsorption for the samples ZIF-8, ZIF-67 and bimetallic material ZIF/Zn-Co at a pressure of 1 atm (Table 3) can be explained by the smaller critical diameter of this gas molecule (3.8 Å) in comparison with the critical diameter of ethane molecule. In this case, the small differences in the rigidity and pore diameter of the cobalt-containing and zinc-containing frameworks have no pronounced effect on the adsorption of methane as compared to that of ethane. However, at pressure increase up to 5 atm and higher (Table 3), the capacity of cobalt-containing adsorbents, first of all, ZIF-67, noticeably exceEDX the capacity of ZIF-8 with Zn^{2+}. Noteworthy, the methane adsorption values exhibited by ZIF-8, ZIF-67 and ZIF-Zn/Co materials are 40% higher than for similar materials described in [6]. Probably, this difference can be explained by the reduced values of specific surface area (1100–1200 m^2/g) of the literature samples [6].

ZIF-67@ZIF-8 composite is characterized by the highest methane capacity in the pressure range of 1–5 atm, despite a slightly reduced value of specific surface area as compared to the monometallic ZIF-8 and ZIF-67 samples, as well as bimetallic ZIF-Zn/Co adsorbent. This phenomenon can be explained by the increased content of cobalt (II) in this sample compared to the bimetallic material ZIF-Zn/Co and the ZIF-67@ZIF-8 composite (Table 1). The possible cooperative effect of simultaneous rotation of MIM "core" and "shell" linkers during the methane adsorption may also contribute to the increase in methane adsorption capacity. A similar phenomenon is described in the literature for low-temperature N_2 adsorption on ZIF-8@ZIF-67 materials [3]. The presence of this effect is supported by the fact that the capacity of the ZIF-67@ZIF-8 sample exceEDX the capacities for methane (25 °C, 1 bar) and, moreover, the sum of capacities of its individual ZIF-8 and ZIF-67 components (Table 3).

The ZIF-8@ZIF-67 composite demonstrates a reduced adsorption capacity for methane as compared to other samples, despite the fact that its specific surface area and total pore volumes are a bit higher than the corresponded characteristics of its ZIF-67@ZIF-8 analog (Table 2). It could be suggested that in this case the cooperative effect associated with the simultaneous rotation of the MIM linkers "core" and "shell" is not realized, due to the less close contact between the domains of ZIF-67 and ZIF-8 [3].

The energetic characteristics are important for the evaluation of potential applications of the studied materials. So, the adsorption isotherms of methane and ethane at different temperatures (0 °C, 50 °C and 75 °C) were measured for ZIF-8 and ZIF-67 samples to evaluate the isosteric heats of adsorption (Fig. 4).

When the temperature is increased from 0 °C to 75 °C, the decrease in the capacity of the ZIF-67 material is about 45% (from 6.67 mmol/g to 3.83 mmol/g at 40 atm) and that of the ZIF-8 adsorbent is 40% (from 5.54 mmol/g to 3.35 mmol/g at 35 atm). The ethane adsorption isotherms in the high pressure region (> 20 atm) for both samples show a sharp increase in the adsorption value, which corresponds to capillary condensation of ethane at this temperature and equilibrium pressure. The obtained isotherms were used to calculate the isosteric heats of adsorption by plotting the corresponding isosteres shown in Fig. 5. It can be seen that the obtained isosteres are linear in the whole range of the studied adsorption values, which allows us to use them to calculate isosteric heats of adsorption.

Based on the calculated adsorption isosteres for methane and ethane, the dependences of isosteric heats of adsorption on the adsorption value were obtained (Fig. 6).

For the ZIF-8 sample, the heat of adsorption was 12.7 ± 0.3 kJ/mol for methane and 23.0 ± 2.1 kJ/mol for ethane (0–75 °C). The ZIF-67 material shows a bit lower heat of adsorption, i.e., 12.1 ± 0.5 kJ/mol for methane and 22.3 ± 2.2 kJ/mol for ethane. Noteworthy, the dependences of the heat of adsorption on the adsorbate filling degree for both materials have the same shape, probably because these materials are isostructural. The maximum on the dependence of the heat of adsorption for ethane (Fig. 6) indicates a presence of "lateral" adsorbate-adsorbate interactions on the surface of both studied adsorbents at significant pore filling degrees [21]. The flat character of this dependence for methane indicates the absence of the above-mentioned interactions between adsorbate molecules. The heat of adsorption for methane on both materials is almost independent of temperature. In contrary, the maximum value for ethane is observed at 0 °C.

There are only limited literature data relevant to the measurements of the heats of adsorption of methane and ethane on the ZIF-8 and ZIF-67 materials. In particular, for the

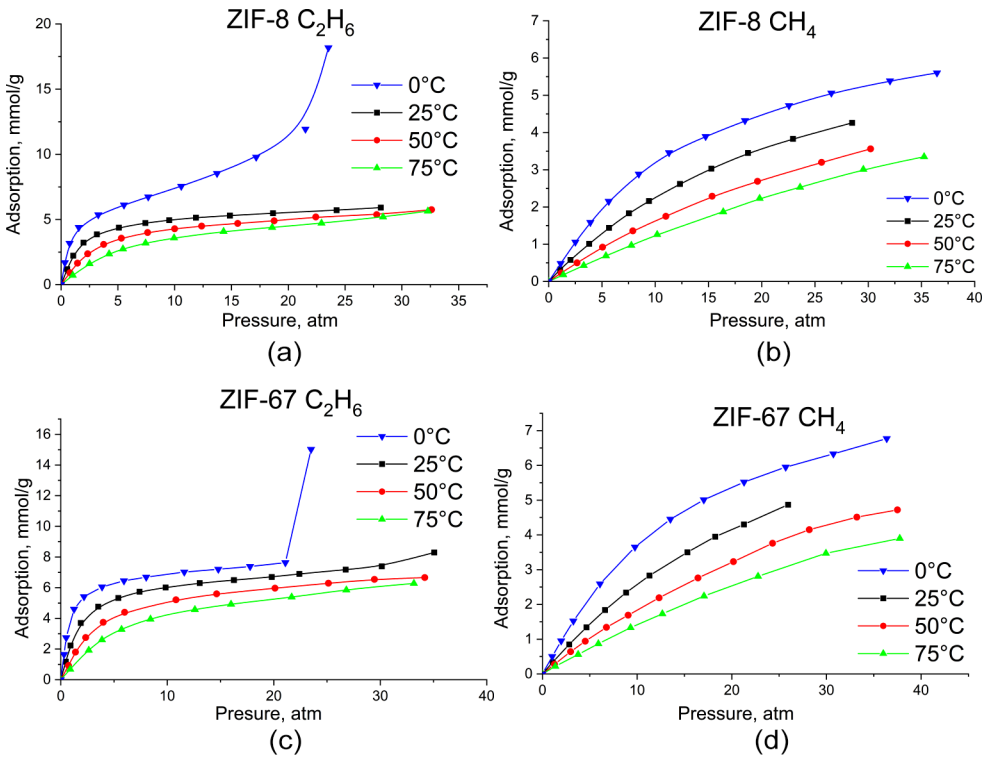

Fig. 4 Adsorption isotherms of methane and ethane at 0, 25, 50 and 75 °C for ZIF-8 (**a**, **b**) and ZIF-67 (**c**, **d**)

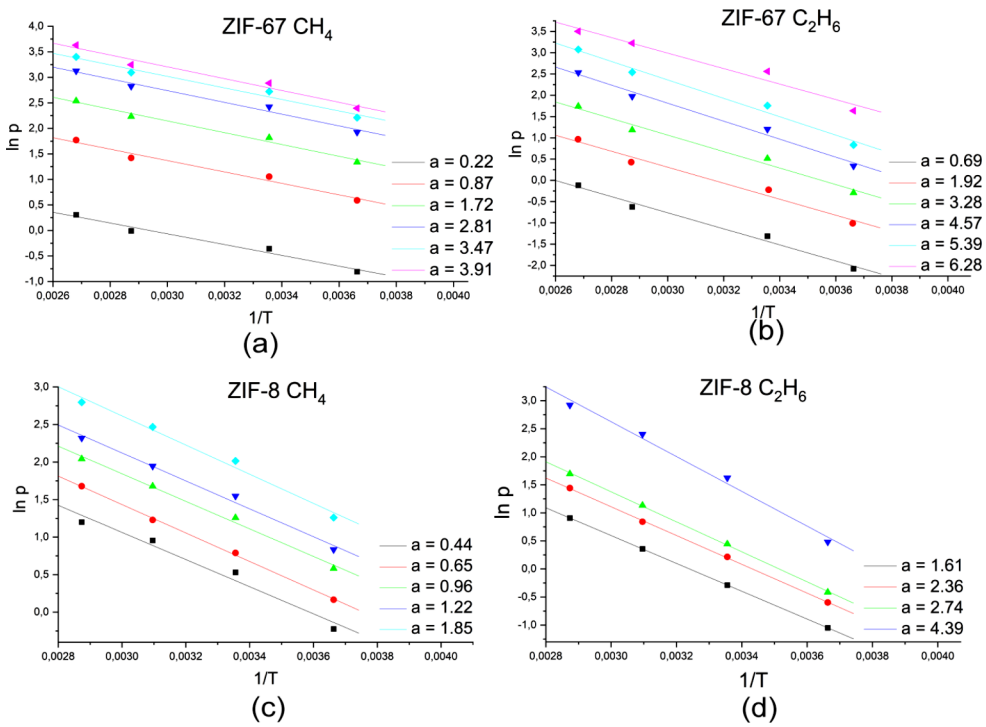

Fig. 5 Methane and ethane adsorption isosteres on ZIF-67 (**a**, **b**) and ZIF-8 (**c**, **d**) at different adsorption values

ZIF-8 system, the heat of adsorption for methane is 13 kJ/mol at the adsorption value of 0.1 mmol/g (25–50 °C) [6], while the heat of adsorption for ethane is 21 kJ/mol at 25 °C (the degree of filling is not specified) [22]. This work results are in a good accordance with the reported values. Noteworthy, the adsorption values for both gases were obtained in this work in a wider temperature range (0–75 °C) and filling degrees as compared to the literature data. Moreover, for ZIF-67, the heat of adsorption values for both gases were obtained for the first time.

Although the adsorption value for both gases on ZIF-67 is higher than that for the ZIF-8 sample, the heats of

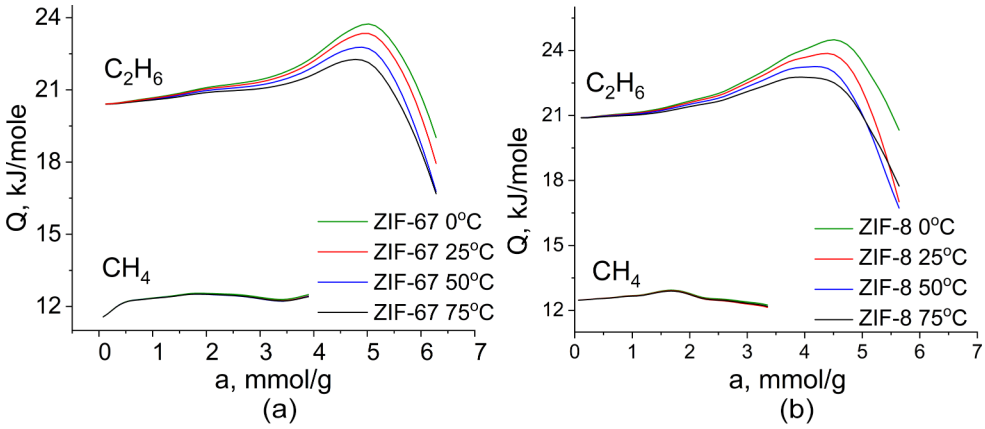

Fig. 6 Dependence of the heat of adsorption of methane and ethane on the adsorption value for ZIF-67 (**a**) and ZIF-8 (**b**)

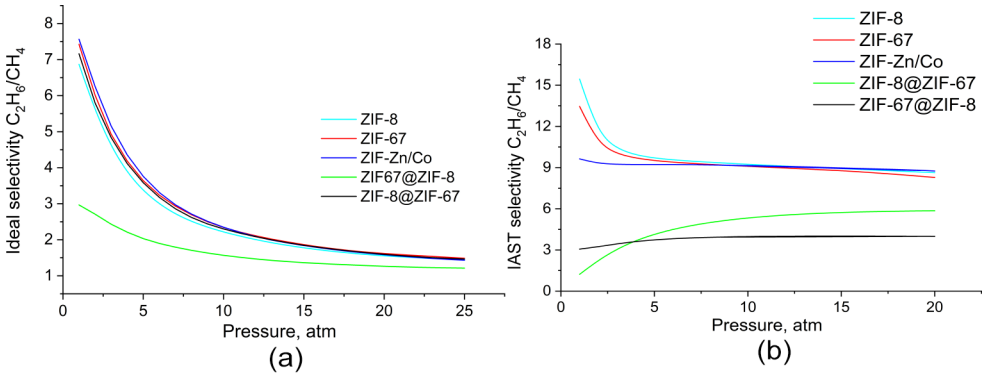

Fig. 7 Pressure dependence of ideal (**a**) and IAST (**b**) selectivity for the C_2H_6/CH_4 pair for the obtained ZIF materials (25 °C)

Table 4 Ideal and IAST selectivities for the obtained ZIF adsorbents (25 °C)

Sample	Ideal selectivity			IAST selectivity at y(CH_4) = 0.9		
	C_2H_6:CH_4, P = 1 atm	C_2H_6:CH_4, P = 5 atm	C_2H_6:CH_4, P = 20 atm	C_2H_6:CH_4, P = 1 atm	C_2H_6:CH_4, P = 5 atm	C_2H_6:CH_4, P = 20 atm
ZIF-8	6.87	3.36	1.55	15.45	9.69	8.63
ZIF-67	7.43	3.64	1.62	13.45	9.51	8.28
ZIF-67@ ZIF-8	2.97	2.03	1.27	1.23	4.15	5.86
ZIF-8@ ZIF-67	7.16	3.58	1.60	3.06	3.73	3.99
ZIF-Zn/ Co (Zn : Co = 1 : 1)	7.57	3.77	1.59	9.64	9.23	8.75

adsorption for methane and ethane are lower. Taking into account that both frameworks are isostructural ones with almost identical textural properties, this difference may be caused by the nature of coordination centers in them: Co^{2+} ions in ZIF-67 and Zn^{2+} ions in ZIF-8. However, a confirmation of this effect requires a further study.

According to the literature, the opposite trends for the adsorption capacity and adsorption heats were observed for carbon dioxide adsorption on ZIF-8 and ZIF-67 materials. For example, for the ZIF-67 sample (S_{BET} = 1478 m^2/g), the heat of adsorption of CO_2 is 9.9 kJ/mol (25–75 °C) [23], while for ZIF-8 (S_{BET} = 1813 m^2/g) it is 19.5 kJ/mol [24] (both papers do not specify the pore filling degree at which these heats of adsorption were calculated). However, its CO_2 capacity is higher (~10.2 mmol/g (40 atm, 25 °C) for ZIF-67 as compared to 8.5 mmol/g for ZIF-8 (40 atm, 25 °C).

For the synthesized ZIF materials, the values of ideal and IAST selectivity for ethane/methane pair were calculated in a wide pressure range (Fig. 7; Table 4).

In the case of IAST selectivity (Fig. 7), the highest values for a mixture of methane and ethane at 1 atm are demonstrated by ZIF-8 (15.5 : 1, 1 atm, 25 °C) and ZIF-67 (13.5 : 1, 1 atm, 25 °C) adsorbents. In the pressure range of 5–20 atm, the bimetallic ZIF-Zn/Co material shows almost identical selectivity value (9.7 : 1, 5 atm, 25 °C) as those

for the monometallic samples, which indicates that, within the frame of the IAST theory, the selectivity value does not depend on the nature of the coordination center in the studied ZIF matrices. When comparing the IAST selectivity values for the "core-shell" composites, it can be seen that in the range of 5–20 atm, this value is the highest for the ZIF-8@ZIF-67 material having zinc-containing "core" (5.86 : 1, 20 atm, 25 °C) in comparison with the selectivity of ZIF-67@ZIF-8 adsorbent with "core" based on Co^{2+} (3.99 : 1, 20 atm, 25 °C).

Regarding the ideal selectivity for the equimolar mixture C_2H_6:CH_4 in the pressure range of 1–25 atm, all materials except the ZIF-67@ZIF-8 composite, show identical values of ideal selectivity. This sample shows a markedly reduced selectivity (2.97 : 1, 1 atm, 25 °C) over the entire range of pressures investigated. This phenomenon could be explained by its increased adsorption capacity for methane.

3 Conclusions

Thus, a series of ZIF materials based on 2-methylimidazolate linkers and with a variable content of Zn^{2+} and Co^{2+} ions in the framework, i.e., monometallic, bimetallic (Zn : Co = 1 : 2, 1 : 1, and 2 : 1), and "core-shell" samples have been synthesized using the original MW-assisted procedures at atmospheric pressure (monometallic and bimetallic samples) and RT-method ("core-shell" composites). These matrices were investigated in the selective adsorption of methane and ethane in a wide range of pressures (1–20 atm) for the first time. A pronounced effect of the coordination center (metal ion) in the framework on the adsorption behavior of the studied samples was found. Thus, Co^{2+}-based adsorbents, i.e., monometallic ZIF-67 sample, bimetallic ZIF-Zn/Co materials and "core-shell" ZIF-67@ZIF-8 composite show increased capacities both for methane and ethane. The highest IAST selectivity (9:1, 15 atm, 25 °C) is shown by the bimetallic ZIF-Zn/Co sample. However, the nature of the coordination center has almost no impact on the ideal selectivity value.

Supplementary Information The online version contains supplementary material available at https://doi.org/10.1007/s10450-024-00505-3.

Author contributions G. S. – Investigation, Writing – original draft, Conceptualization. V. I. - Text Editing, Conceptualization, Data CurationKravtsov L. A., Glukhov L. M., Arkhipov D. A. – Material Synthesis, Investigation. V. V. and G. I. - Material CharacterizationKustov L. M. - Text Review and Editing, ConceptualizationAll authors reviewed the finished manuscript.

Funding This work was supported by the Russian Science Foundation (grant 23-73-30007).

Data availability No datasets were generated or analysed during the current study.

Declarations

Ethical statements - It is not applicable.

Competing interests The authors declare no competing interests.

References

1. Rowsell, J.L.C., Spencer, E.C., Eckert, J., Howard, J.A.K., Yaghi, O.M. Gas Adsorption Sites in a Large-Pore Metal-Organic Framework //, Science: — 2005. — V. 309. — № 5739. — P. 1350–1354. (1979)
2. Yuan, S.H., Isfahani, A.P., Yamamoto, T., Muchtar, A., Wu, C.Y., Huang, G., You, Y.C., Sivaniah, E., Chang, B.K., Ghalei, B.: Nanosized Core–Shell Zeolitic Imidazolate frameworks-based membranes for gas separation // small methods. — 2020. — V. 4. — № 8.
3. Loloei, M., Kaliaguine, S., Rodrigue, D.: CO2-Selective mixed matrix membranes of bimetallic Zn/Co-ZIF vs. ZIF-8 and ZIF-67 // Sep Purif Technol. — 2022. — V. 296. — P. 121391.
4. Krokidas, P., Castier, M., Economou, I.G.: Computational Study of ZIF-8 and ZIF-67 Performance for Separation of Gas Mixtures // The Journal of Physical Chemistry C. — — V. 121. — № 33. — P. 17999–18011. (2017)
5. Kolokolov, D.I., Stepanov, A.G., Jobic, H.: Mobility of the 2-Methylimidazolate Linkers in ZIF-8 Probed by ^{2} H NMR: Saloon Doors for the Guests // The Journal of Physical Chemistry C. —. — V. 119. — № 49. — P. 27512–27520. (2015)
6. Awadallah, -F.A., Hillman, F., Al-Muhtaseb, S.A., Jeong, H.-K.: Adsorption of Carbon Dioxide, Methane, and Nitrogen Gases onto ZIF Compounds with Zinc, Cobalt, and Zinc/Cobalt Metal Centers // J Nanomater. — 2019. — V. 2019. — P. 1–11
7. Hillman, F., Zimmerman, J.M., Paek, S.-M., Hamid, M.R.A., Lim, W.T., Jeong, H.-K.: Rapid microwave-assisted synthesis of hybrid zeolitic–imidazolate frameworks with mixed metals and mixed linkers // J Mater Chem A Mater. — 2017. — V. 5. — № 13. — P. 6090–6099
8. Pan, Y., Sun, K., Liu, S., Cao, X., Wu, K., Cheong, W.-C., Chen, Z., Wang, Y., Li, Y., Liu, Y., Wang, D., Peng, Q., Chen, C., Li, Y.: Core–Shell ZIF-8@ZIF-67-Derived CoP Nanoparticle-Embedded N-Doped Carbon Nanotube Hollow Polyhedron for Efficient Overall Water Splitting // J Am Chem Soc. — — V. 140. — № 7. — P. 2610–2618. (2018)
9. Fujiwara, A., Watanabe, S., Miyahara, M.T.: Flow Microreactor Synthesis of Zeolitic Imidazolate Framework (ZIF)@ZIF Core–Shell Metal–Organic Framework Particles and Their Adsorption Properties // Langmuir. — — V. 37. — № 13. — P. 3858–3867. (2021)
10. Panchariya, D.K., Rai, R.K., Anil Kumar, E., Singh, S.K.: Core–Shell Zeolitic Imidazolate Frameworks for Enhanced Hydrogen Storage // ACS Omega. — 2018. — V. 3. — № 1. — P. 167–175
11. Kachala, V.V., Khemchyan, L.L., Kashin, A.S., Orlov, N.V., Grachev, A.A., Zalesskiy, S.S., Ananikov, V.P.: Target-oriented analysis of gaseous, liquid and solid chemical systems by mass spectrometry, nuclear magnetic resonance spectroscopy and electron microscopy // Russian Chemical Reviews. — 2013. — V. 82. — № 7. — P. 648–685
12. Kashin, A.S., Ananikov, V.P.: A SEM study of nanosized metal films and metal nanoparticles obtained by magnetron sputtering

// Russian Chemical Bulletin. — — V. 60. — № 12. — P. 2602–2607. (2011)
13. Deyko, G.S., Glukhov, L.M., Isaeva, V.I., Chernyshev, V.V., Vergun, V.V., Archipov, D.A., Kapustin, G.I., Tkachenko, O.P., Nissenbaum, V.D., Kustov, L.M. Modifying HKUST-1 Crystals for Selective Ethane Adsorption Using Ionic Liquids as Synthesis Media //, Crystals: (Basel). — 2022. — V. 12. — № 2. — P. 279
14. Tsivadze, A.Y., Aksyutin, O.E., Ishkov, A.G., Fomkin, A.A., Men'shchikov, I.E., Pribylov, A.A., Isaeva, V.I., Kustov, L.M., Shkolin, A.V., Strizhenov, E.M.: Adsorption of methane on an MOF-199 organometallic framework structure at high pressures in the range of supercritical temperatures // Protection of Metals and Physical Chemistry of Surfaces. — — V. 52. — № 1. — P. 24–29. (2016)
15. Myers, A.L., Prausnitz, J.M.: Thermodynamics of mixed-gas adsorption // AIChE Journal. — 1965. — V. 11. — № 1. — P. 121–127
16. Fraux, G., Boutin, A., Fuchs, A.H., Coudert, F.-X.: On the use of the IAST method for gas separation studies in porous materials with gate-opening behavior // Adsorption. — — V. 24. — № 3. — P. 233–241. (2018)
17. Pawley, G.S.: Unit-cell refinement from powder diffraction scans // J Appl Crystallogr. — 1981. — V. 14. — № 6. — P. 357–361
18. Zlokazov, V.B., Chernyshev, V.V., MRIA -: A Program for a Full Profile Analysis of Powder Neutron-Diffraction Time-of-Flight (Direct and Fourier) Spectra // Materials Science Forum. — 1991. — V. 79–82. — P. 283–288
19. Kida, K., Okita, M., Fujita, K., Tanaka, S., Miyake, Y.: Formation of high crystalline ZIF-8 in an aqueous solution // CrystEngComm. —. — V. 15. — № 9. — P. 1794. (2013)
20. Isaeva, V.I., Papathanasiou, K., Chernyshev, V.V., Glukhov, L., Deyko, G., Bisht, K.K., Tkachenko, O.P., Savilov, S.V., Davshan, N.A., Kustov, L.M.: Hydroamination of Phenylacetylene with Aniline over Gold Nanoparticles Embedded in the Boron Imidazolate Framework BIF-66 and Zeolitic Imidazolate Framework ZIF-67 // ACS Appl Mater Interfaces. — 2021. — V. 13. — № 50. — P. 59803–59819
21. Rouquerol, F., Rouquerol, J., Sing, K.S.W.: Thermodynamics of Adsorption at the Gas/Solid Interface // Adsorption by Powders and Porous Solids. Elsevier, — — P. 25–56. (2014)
22. Wu, Y., Chen, H., Liu, D., Qian, Y., Xi, H.: Adsorption and separation of ethane/ethylene on ZIFs with various topologies: Combining GCMC simulation with the ideal adsorbed solution theory (IAST) // Chem Eng Sci. — — V. 124. — P. 144–153. (2015)
23. Ethiraj, J., Palla, S., Reinsch, H.: Insights into high pressure gas adsorption properties of ZIF-67: Experimental and theoretical studies // microporous and mesoporous materials. — 2020. — V. 294. — P. 109867.
24. Castro, A., Jardim, E., Reguera, E.: CH4 and CO2 Adsorption Study in ZIF-8 and Al-BDC MOFs // IX Congreso de Ciencias, Tecnología e Innovación Química QUIMICUBA. Habana, Cuba, — — P. 1–20. (2015)